Analytical Modeling of VTEC and STEC via Altitudinal Integration of Solar Radiation Power Density

1. Abstract

This article focuses on determining VTEC and STEC values at any geographic location. This determination is achieved not through satellite data, but via a robust theoretical framework. The method employed involved developing a formula for electron volume density. This density is derived from expressions describing the altitudinal variation of solar radiation power, volume, and the ionization energy of the oxygen atom. The resulting formula was obtained after adjusting the initial formula, which yielded exponential values at 6 AM, 12 PM, 6 PM, and midnight. Thus, for a given geographic location, the formula provides the VTEC and STEC values, as well as their diurnal variability curves. The VTEC/STEC modeling reveals the following key aspects: (1) For a given longitude, the variability of VTEC/STEC with latitude highlights the inverse fountain effect at 6 AM and 6 PM, with amplitudes decreasing with distance from the equator at latitudes of 10°N,S to 20°N,S. At other times of day, the amplitudes increase from the equator to the North and South Poles, where the observed VTEC/STEC values are exponential. (2) For a given latitude, the modeling based on longitude provides diverse profiles. (3) Also, if the vertical drift velocity is varied via the production factor, the following observations are made: (a) The higher the drift velocity or production factor, the lower the VTEC/STEC values. (b) The lower these factors are, the higher the VTEC/STEC values. Other applications include, firstly, the development of formulas for modeling critical frequencies and electric current density. Secondly, the introduction of another form of VTEC, STEC, whose unit is the TECU, equal to 10^{16} electrons per meter. Finally, future research will focus on polar electron jets, scintillations, electric and magnetic fields, and the magnetosphere.

.***Keywords:*** *Theoretical framework; VTEC; STEC; volume density; ionization energy; production factor; drift velocity; production factor.*

2. Introduction

The TEC, or Total Electron Content, is a key parameter of the ionosphere for precise satellite positioning and location. The TEC varies over time and space, and for a given geographic location, it also varies seasonally and is correlated with the sunspot cycle. Therefore, the TEC will be the subject of several studies to understand, among other things, equatorial ionization anomalies (Scherliess & Fejer, 1999; Rishbeth et al., 2000). These anomalies are characterized by a trough-like structure at maximum NmF2 ionization densities and a dome-like structure at maximum HmF2 heights or altitudes centered at the equator. Karia, S.P., et al. have also studied the detection of earthquake precursors. (2014), better absorb the impacts of scintillations (Surendra Sunda et al, 2013) on GNSS etc. The TEC briefly described is obtained after processing from a system consisting of a constellation of satellites, multiple ground control stations and receivers. Such a system is known by the generic term GNSS (Global Navigation Satellite System), which includes specific versions such as GPS for Americans, Galileo for Europeans, GLONASS for Russians, and BeiDou for Chinese. The inherent uncertainty of obtaining TEC data is well-established and not the only factor. While TEC data can be obtained, it is unfortunately not available for every geographic location. Even at locations where it is possible, temporal discontinuities and biases may be observed due to the inherent variability of the stations or satellites. In addition to these in-situ measurements, TEC prediction models have been developed and are accessible via internet platforms such as IRI 2020, NeQuick, TIEGCM, etc. However, these models remain limited because, besides the predictive quality, the lack of data quickly becomes apparent due to internet outages or platform malfunctions. What alternative is there in the face of such a contingency? What theoretical basis underpins the variability of the various ionospheric parameters? This is where the proposed theoretical framework comes in. Indeed, the analytical calculation of VTEC and STEC by altitudinal integration of solar radiation power density is a model that allows for the theoretical calculation and modeling of VTEC and STEC at any geographical location. It is an endogenous model but still requires a broad range of knowledge to function However, once programmed, simply entering the desired latitude and longitude is enough to generate the VTEC and STEC values, both in terms of data and graphs. The altitudinal integration calculation, besides its theoretical nature and therefore its accessibility, is also a model that could be implemented, similar to IRI 2020 or NeQuick, or even more simply on a computer or laptop. Therefore, the development section will explain the methodology behind the theoretical calculation of VTEC and STEC, highlighting the necessary nuances that led to the validation of the formula and its importance as a predictive tool. Beyond VTEC and STEC, it will also consider other parameters such as critical frequencies (foF2), current densities, etc. Finally, after outlining the future prospects, the conclusion will summarize the key findings of the study.

3. Methodology

The objective of this article was to propose a robust theoretical framework for modeling the variations of both VTEC and STEC at any geographical location. This framework was formalized starting from the altitudinal integration of the electron volume density, which was initially neither straightforward nor easy to achieve. However, this will be possible, firstly through the development of altitudinal expressions for the solar radiation power and the ionization volume, which will allow the calculation of the solar radiation power density (W/m³). Thus, from this knowledge, and in conjunction with that of the ionization energy of the oxygen atom or other atoms, the electron volume density (e/m³) at a given altitude will be determined, and from its altitudinal integration, the VTEC and STEC will be calculated at a given geographical location. The essential steps are as follows:

3.1. Analytical calculations of surface and volume power density

3.1.1. Altitudinal expression of the ionization densification surface

The ionization densification surface [1] is the surface through which electromagnetic waves are reflected at a given critical frequency. Knowing the expression for its temporal variability by the product of the coordinates $x(t)$ and $y(t)$ we can therefore find its altitudinal variation as a function of z as follows:

$$\begin{cases} \dfrac{dS(x,y)}{dz} = \dfrac{dS(x,y)}{dt} \times \dfrac{dt}{dz} \\ \dfrac{dS(x,y)}{dz} = \dfrac{\mathrm{V}x(t).y(t) + \mathrm{V}y(t).x(t)}{Vz(t)} \rightarrow Vz(t) \neq 0 \end{cases}$$

$Vz(12H) = 0$ If we consider only three decimal places, then we can deduce that the altitudinal variation of the ionization densification surface remains to be determined at this time, either by assumptions or by other methods. At a given hour or timet_0 given or fixed other than 12 PM, $dS(x,y)/dz$ is a constant from which, by integration, we recover the altitudinal expression for the ionization densification surface. Its expression is given by:

$$\begin{cases} Vz(t) \neq 0 \rightarrow S_{(x,y)}(z) = \left[\dfrac{dS(x,y)}{dz}\right]_{t0} z + cste \rightarrow cste = S_{(x,y)}(z_0) - \left[\dfrac{dS(x,y)}{dz}\right]_{t0} z_0 \\ S_{(x,y)}(z) = (z - z_0)\left[\dfrac{dS(x,y)}{dz}\right]_{t0} + S_{(x,y)}(z_0) \quad (1) \end{cases}$$

3.1.2. Altitudinal expression of the ionization volume

By analogy with the ionization densification surface, we find the altitudinal expression of the ionization volume at a fixed time.

$$\begin{cases} \dfrac{dV(x,y,z)}{dz} = \dfrac{dV(x,y,z)}{dt} \times \dfrac{dt}{dz} \\ \dfrac{d[S(x,y).z]}{dz} = \dfrac{[\mathrm{V}x(t).y(t) + \mathrm{V}y(t).x(t)].z(t) + S(x,y).Vz(t)}{Vz(t)} \rightarrow Vz(t) \neq 0 \\ \dfrac{dV(x,y,z)}{dz} = \dfrac{dS(x,y)}{dz}.z + S(x,y) \\ V_{(x,y,z)}(z) = (z - z_0)\left[\dfrac{dS(x,y)}{dz}.z + S(x,y)\right]_{t0} + V_{(x,y,z)}(z_0) \qquad (2) \end{cases}$$

3.2. Analytical calculations of the power density of solar radiation

3.2.1. Altitudinal expression of solar radiation power

The temporal expression of the power of solar radiation $P_0(t)$ by Segda et al. (2023a), (2023b) knowing the altitudinal expression of the ionization densification surface.

$$\begin{cases} \dfrac{dkP0(t)}{dz} = \dfrac{dkP0(t)}{dt} \times \dfrac{dt}{dz} \rightarrow \dfrac{dkP0(t)}{dz} = \dfrac{h(t)}{V_z(t)} \\ kP0(z) = \left[\dfrac{h}{V_z}\right]_{t0} z + cste \rightarrow cste = kP0(z_0) - \left[\dfrac{h}{V_z}\right]_{t0} z_0 \rightarrow P_0(t) = 2\sin\left(\dfrac{\pi}{12}t\right)\cos\left(\dfrac{\pi}{6}t\right) \\ kP0(z) = \left[\dfrac{h}{V_z}\right]_{t0}(z - z_0) + kP0(z_0) \ (3) \end{cases}$$

In this formula from Segda et al. (2025) « k » is the ionization production factor. This factor has a latitude λ The given value is obtained from the average daily velocity of the vertical ionization drift velocity using the formula:

$$V_{pz}(\lambda, k)_{moy} = 36{,}70.10^{-2}.k.sin\lambda \ (4)$$

For modeling purposes, the average ionization drift rate is approximately $20{,}60\ m.s^{-1}$ will be considered. For example, according to Segda et al. (2026), on 13/09/2025, the production factor obtained from the 2020 IRI for the city of Singapore (LAT 1.28° and LONG 103.85°E), considered to be the closest city to the equator, was $k_{Sing} = 2511{,}54$. Such a factor of production is deduced from an average vertical drift speed of $20{,}59\ m.s^{-1}$.

3.2.2. Altitudinal expression of the surface power density (W/m2) of solar radiation

Given that the altitudinal expressions for both the ionization densification surface and the power of solar radiation are known, the expression for the surface power density (W/m2) of solar radiation can be deduced as follows:

$$\begin{cases} D_p(z) = \dfrac{kP0(z)}{S_{(x,y)}(z)} \\ D_p(z) = \dfrac{\left[\dfrac{h}{V_z}\right]_{t0}(z - z_0) + kP0(z_0)}{\left[(z - z_0)\left[\dfrac{dS(x,y)}{dz}\right]_{t0} + S_{(x,y)}(z_0)\right]} \end{cases} \rightarrow (5)$$

In this expression, the points of indeterminacy are the points where the density surface as a function of altitude becomes zero. A priori, these are 6 AM and 6 PM, where their surfaces were already zero to within a few decimal places. The corresponding altitudes for the other hours are given by the following expression:

$$z = \frac{z_0\left[\dfrac{dS(x,y)}{dz}\right]_{t0} - S_{(x,y)}(z_0)}{\left[\dfrac{dS(x,y)}{dz}\right]_{t0}}$$

After further calculations for the 6 AM and 6 PM points, we find 22 points with altitudes ranging from -100m to 100m.

Finally, the altitudinal integration of the surface power density will not give us the equivalent of the TEC (the number of electrons per square meter), but rather another form of the TEC: linear density, or the number of electrons per meter.

3.2.3. Altitudinal expression of the volumetric power density (W/m³) of ionization

$$D_p(z) = \frac{\left[\frac{h}{V_z}\right]_{t0}(z - z_0) + kP0(z_0)}{\left[(z - z_0)\left[\frac{dS(x,y)}{dz}.z + S(x,y)\right]_{t0} + V_{(x,y,z)}(z_0)\right]} \quad (6)$$

The altitudinal integration of the volumetric power density will give us the equivalent of the TEC, that is to say the number of electrons per square meter.

3.3. Ionization energy

First ionization energy E_{1i} of the oxygen atom being$1421k\text{J}.mol^{-1}$ The corresponding energy for an oxygen atom is then obtained by dividing the first ionization energy by Avogadro's number $\mathcal{N}_A$. Avogadro's number is defined, with respect to the mole of oxygen atoms, as the grouping of « $6{,}0221408.10^{23}$» oxygen atoms. Thus, the ionization energy obtained from the oxygen atom is:

$$\frac{E_{1i}}{\mathcal{N}_A} = 2{,}36\ 10^{-18}\text{J} \quad (7)$$

Surface or volume power density is expressed in W/m² or W/m³, respectively, and watts are equivalent to joules per second, or J/s. Thus, knowing the ionization energy of an atom, one can determine the number of electrons corresponding to a power density at a specific altitude z. However, in addition to the oxygen atom, other chemical species exhibit power density variations with altitude, as shown in Figure 1 below, extracted from Banks et al., 1976.

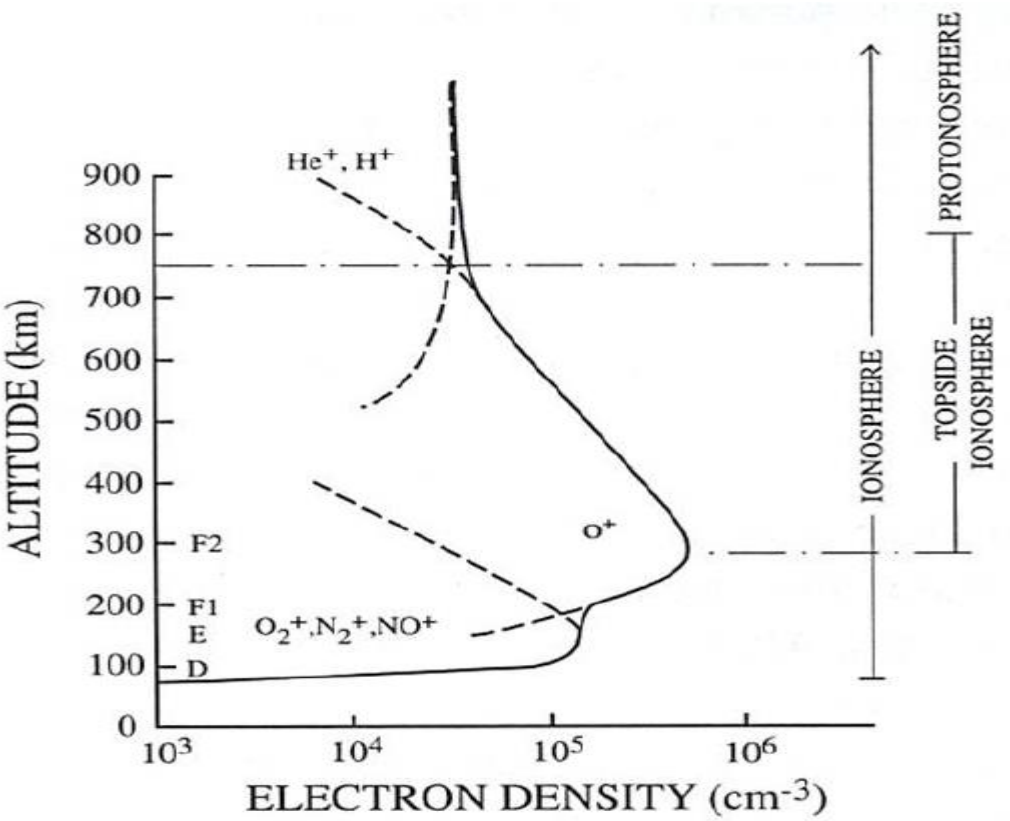

Fig.1. Representative ion density profiles for the daytime middle-latitude ionosphere showing the layered structure (D; E; F1, and F2) **[**Banks et al., 1976**]**.

3.4. Surface and volume electron density at altitude z in TECU

3.4.1. Surface electron density at altitude z in TECU

The surface electron density in TECU will be obtained by dividing the number of atoms or electrons by 1 TECU, i.e., multiplying by 10^{-16}. The number of atoms or electrons per square meter is obtained by multiplying the power density per square meter by the inverse of the ionization energy of an atom.

$$\mathrm{N(z)} = \frac{\mathcal{N}_A}{E_{1i}}\,\mathrm{Dp}.\times 10^{-16} \rightarrow 42{,}8.\,\mathrm{Dp}$$

However, if we consider that this is an hourly variation, we must also divide by 3600. Thus, the surface electron density at a given altitude z and time is given by the formula:

$$\begin{cases} \mathrm{N(z)} = \left(\dfrac{42{,}38}{3600}\right).\mathrm{Dp} \rightarrow \\ \mathrm{N(z)} = \left(\dfrac{42{,}38}{3600}\right).\dfrac{\left[\dfrac{h}{V_z}\right]_{t0}(z-z_0) + kP0(z_0)}{\left[(z-z_0)\left[\dfrac{dS(x,y)}{dz}\right]_{t0} + S_{(x,y)}(z_0)\right]} \end{cases} \qquad \mathrm{TECU} \rightarrow 10^{16} e.m^{-2}\ (8)$$

This method gives us the electron density per m² at altitude z, expressed in TECU units, where 1 TECU equals $10^{16} e.m^{-2}$. However, its integration or summation between two altitudes $\mathrm{VTEC\ U(\Delta z)}$ will not give the equivalent of VTEC in the broad sense of the term, but of the number of electrons per meter, which we will denote $\mathrm{VTEC\ U(\Delta z)}_{line}$.

3.4.2. Electron volume density at altitude z in TECU

$$\mathrm{N(z)} = \left(\frac{42{,}38}{3600}\right)\frac{\left[\dfrac{h}{V_z}\right]_{t0}(z-z_0) + kP0(z_0)}{\left[(z-z_0)\left[\dfrac{dS(x,y)}{dz}.z + S(x,y)\right]_{t0} + V_{(x,y,z)}(z_0)\right]}\mathrm{TECU} \rightarrow 10^{16} e.m^{-3}\ (9)$$

3.5. Conventional VTEC and Linear VTEC

3.5.1. Linear VTEC or other form of VTEC or STEC

The linear electron density represents the number of electrons per square meter integrated along the path of a satellite-receiver signal through the ionospheric layer. However, this is not the same as conventional VTEC or STEC.

$$\mathrm{VTEC\ U(\Delta z)}_{line} = \int_{z1}^{z2} N(z)dz = \left(\frac{42{,}38}{3600}\right).\int_{z1}^{z2}\frac{\left[\dfrac{h}{V_z}\right]_{t0}(z-z_0) + kP0(z_0)}{\left[(z-z_0)\left[\dfrac{dS(x,y)}{dz}\right]_{t0} + S_{(x,y)}(z_0)\right]}dz$$

Which is of the form:

$$\begin{cases} \displaystyle\int_{z1}^{z2}\frac{az+b}{cx+d}dz \\ a = \left[\dfrac{h}{V_z}\right]_{t0} \rightarrow b = kP0(z_0) - \left[\dfrac{h}{V_z}\right]_{t0} z_0 \\ c = \left[\dfrac{dS(x,y)}{dz}\right]_{t0} \rightarrow d = S_{(x,y)}(z_0) - \left[\dfrac{dS(x,y)}{dz}\right]_{t0} z_0 \end{cases}$$

After integration, we find the expression that must be expressed in absolute value for negative values:

$$\mathrm{VTEC\ U(\Delta z)}_{line} = \left(\frac{42{,}38}{3600c}\right).\left(\left[(az_2+b) - a\left(\frac{cz_2+d}{c}\right)\right]ln|cz_2+d| + \left[a\left(\frac{cz_1+d}{c}\right) - (az_1+b)\right]ln|cz_1+d| + a(z_2-z_1)\right)\ (10)$$

Figure 2 below gives an example of variability at latitude 13°N,S and longitude 358°E

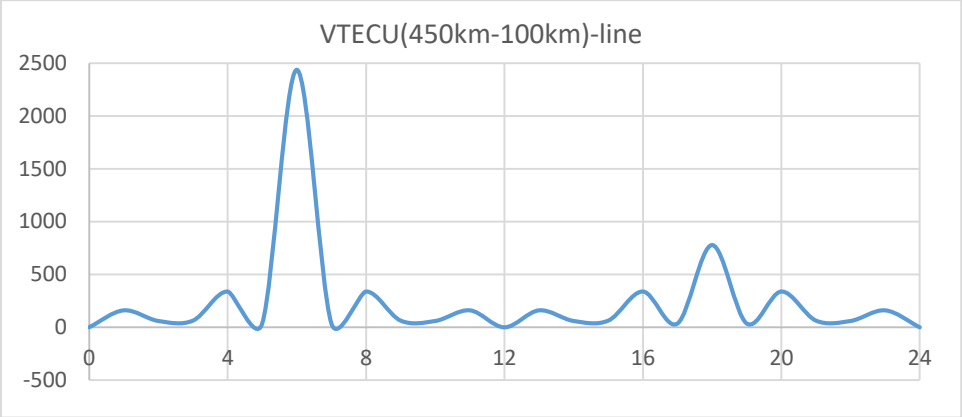

Fig.2. Electron density in 1016 electrons/m from altitude of 450km to 100km and at geographical position LAT 13° and LONG 358°E with the value of noon 12H exponential but taken as zero on the graph.

3.5.2. Conventional VTEC

$$\text{VTEC U}(\Delta z) = \int_{z1}^{z2} N(z)dz = \left(\frac{42{,}38}{3600}\right) \int_{z1}^{z2} \frac{\left[\frac{h}{V_z}\right]_{t0}(z - z_0) + kP0(z_0)}{\left[(z - z_0)\left[\frac{dS(x,y)}{dz}.z + S(x,y)\right]_{t0} + V_{(x,y,z)}(z_0)\right]} dz$$

The integration yielding the VTEC is of the form:

$$\begin{cases} \int_{z1}^{z2} \frac{az + b}{cz + c} dz \\ a = \left[\frac{h}{V_z}\right]_{t0} \rightarrow b = kP0(z_0) - \left[\frac{h}{V_z}\right]_{t0} z_0 \\ c = \left[\frac{dS(x,y)}{dz}.z + S(x,y)\right]_{t0} \rightarrow d = V_{(x,y,z)}(z_0) - \left[\frac{dS(x,y)}{dz}.z + S(x,y)\right]_{t0} z_0 \end{cases}$$

After integration, we find the expression or where we must use absolute values for negative values:

$$\text{VTEC U}(\Delta z) = \left(\frac{42{,}38}{3600c}\right).\left(\left[(az_2 + b) - a\left(\frac{cz_2 + d}{c}\right)\right] ln|cz_2 + d| + \left[a\left(\frac{cz_1 + d}{c}\right) - (az_1 + b)\right] ln|cz_1 + d| + a(z_2 - z_1)\right) \quad (11)$$

The following graphs are obtained from Figure 3 below as an example for a layer of 450 to 100km.

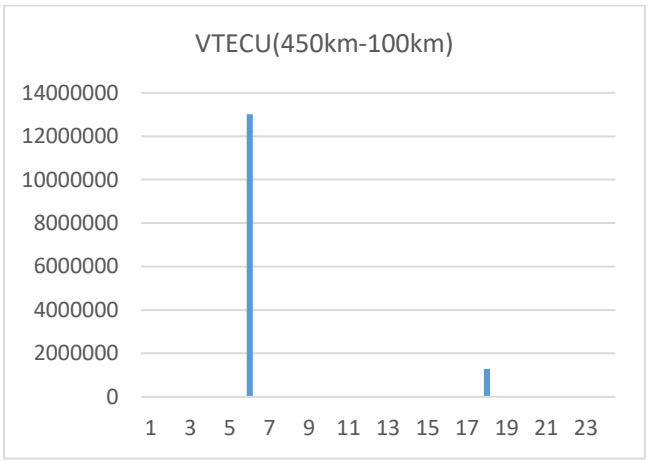

VTECU with all values. The VTECU values observed at 6 AM and 6 PM are exponential values compared to other times.

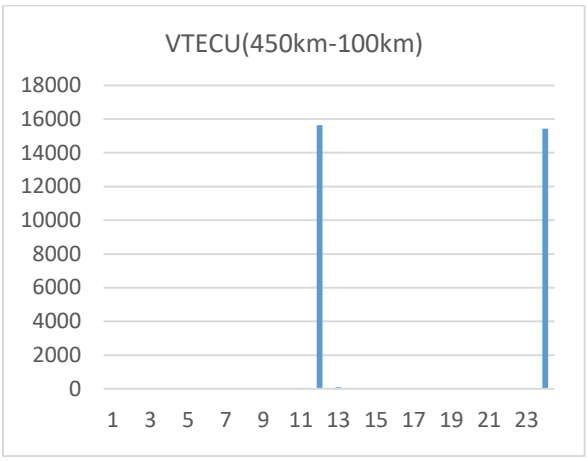

VTECU values at 6 AM and 6 PM are taken as zero. Exponential values relative to other times are observed at 12 PM and 12 AM.

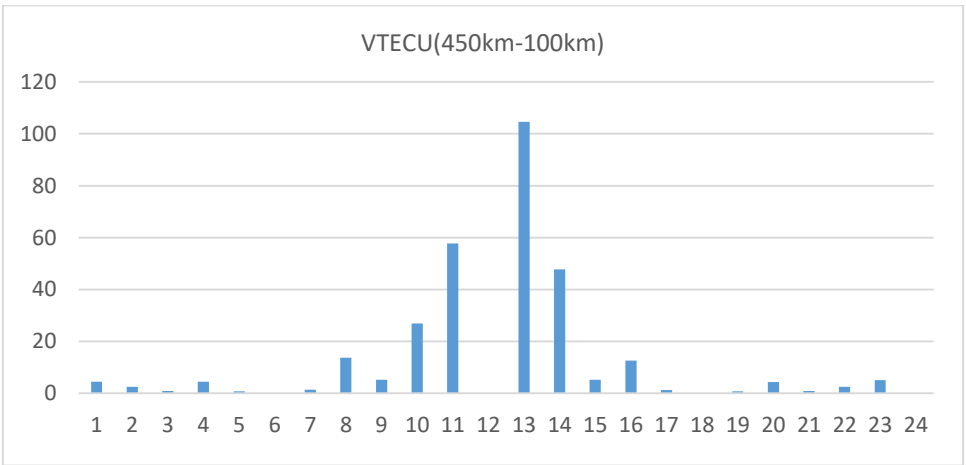

VTECU values at 6 AM, 6 PM, 12 PM, and 12 AM are considered zero. VTECU values at other times are recorded.

Fig.3. Histogram graphs of VTEC variability at LAT 13°N or S, LONG 358°E

Thus we obtain the VTECU variability curve in Figure 4 below where the values at 6H, 18H, 12H and 24H are taken as zero.

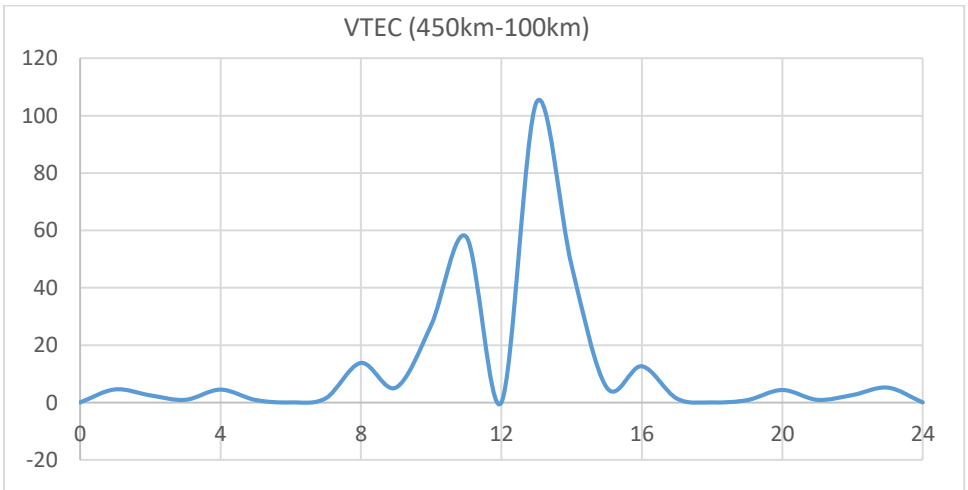

Fig.4.Variability of VTECU at the position LAT 13° North and LONG 358°E or the value at 6H, 12H, 18H and 24H exponential are taken as zero.

4. Results

This results section is a table summarizing a key part of the findings based on the methodology. The remaining results will be presented and discussed in the discussion section.

Table 1. Presentation of some results

Electron volume density at altitude z in TECU

$$\mathrm{N(z)} = \left(\frac{42{,}38}{3600}\right)\frac{\left[\frac{h}{V_z}\right]_{t0}(z - z_0) + kP0(z_0)}{\left[(z - z_0)\left[\frac{dS(x,y)}{dz}.z + S(x,y)\right]_{t0} + V_{(x,y,z)}(z_0)\right]}\mathrm{TECU} \rightarrow 10^{16}e.m^{-3} \quad (9)$$

Conventional VTEC

$$\mathrm{VTEC\ U(\Delta z)} = \int_{z1}^{z2} N(z)dz$$

$$\mathrm{VTEC\ U(\Delta z)} = \left(\frac{42{,}38}{3600c}\right).\left(\left[(az_2 + b) - a\left(\frac{cz_2 + d}{c}\right)\right]ln|cz_2 + d| + \left[a\left(\frac{cz_1 + d}{c}\right) - (az_1 + b)\right]ln|cz_1 + d| + a(z_2 - z_1)\right) \quad (11)$$

$$a = \left[\frac{h}{V_z}\right]_{t0} \rightarrow b = kP0(z_0) - \left[\frac{h}{V_z}\right]_{t0} z_0$$

$$c = \left[\frac{dS(x,y)}{dz}.z + S(x,y)\right]_{t0} \rightarrow d = V_{(x,y,z)}(z_0) - \left[\frac{dS(x,y)}{dz}.z + S(x,y)\right]_{t0} z_0$$

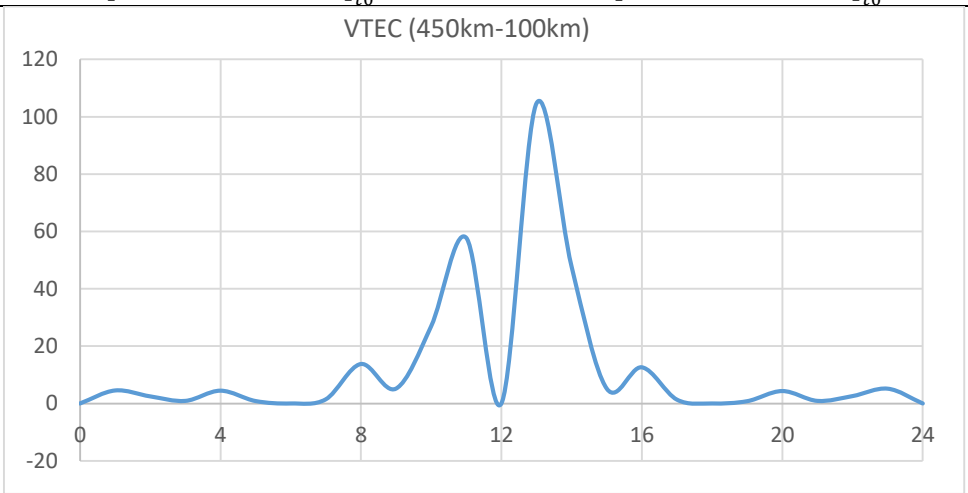

Fig.4.Variability of VTECU at the position LAT 13° North and LONG 358°E or the value at 6H, 12H, 18H and 24H exponential are taken as zero.

5. Discussion

5.1. Context: Approach using time measurement of satellite clocks and receivers

The TEC, or Total Electron Content, represents the number of electrons per cubic meter integrated along the path of a satellite-receiving signal through the ionospheric layer. The TEC therefore represents the number of electrons per square meter and consequently the electron density along a tube with a cross-section of one square meter, symbolizing the signal. It is given by the formula:

$$\int \mathrm{N}ds \;\rightarrow\; N(e.m^{-3}); ds(m) \quad (12)$$

The TEC is expressed in TECUs, where 1 TECU equals 10^{16} electrons/m². The TEC is determined in practice (Figure 5) using the propagation delay of signals from a dual-frequency satellite $f_1 = 1575{,}42Hz$ and $f_2 = 1227{,}6Hz$ to a receiver, all based on the theory of radio wave propagation through the plasma, which is the ionosphere.

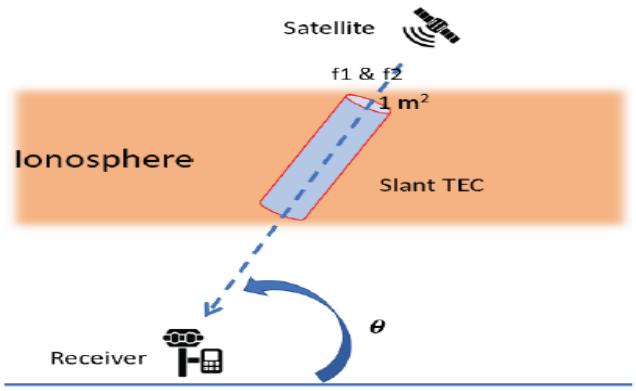

Fig.5. Slant total electron content (STEC) illustration (Phyo et al., 2023)

The TEC thus defined represents the oblique TEC, specifically called the STEC or Slant TEC. Reduced to its vertical equivalent, the STEC, the TEC will be called the VTEC or Vertical TEC. The STEC and the VTEC are related by the equation below, where "e" is the satellite's elevation angle and h is the reference ionospheric height:

$$VTEC = \left[1 - \left(\frac{\cos e}{1 + \frac{h}{R_T}}\right)^2\right] STEC \quad (13)$$

Indeed, according to the theory, every electromagnetic wave propagates along a direction of propagation characterized by a vector called the wave vector $\vec{k}$ also called the dispersion relation. This relation is given by the following formula below if, for example $\overrightarrow{u_z}$ is a unit vector indicating the direction of propagation and n the refractive index of the medium:

$$\vec{k} = \frac{\omega}{\mathrm{V}} \overrightarrow{u_z} = n \frac{\omega}{\mathrm{C}} \overrightarrow{u_z} \quad (14)$$

With ω and V respectively represent the angular frequency and velocity of the wave in the propagation medium with refractive index n. Thus, if the propagation or traversal medium is the ionosphere, then the dispersion relation is given by the formula below, where ω_p is the plasma pulse:

$$k^2 = \frac{\omega^2 - {\omega_p}^2}{C^2} \; et \; \omega_p = \sqrt{\left(\frac{{q_p}^2}{m_p \varepsilon_0}\right) N} \quad (15)$$

This plasma pulsation is highly dependent on the characteristics of the electrons, which have greater mobility due to their extremely low mass compared to positive or negative ions. Therefore, the plasma pulsation will be

approximated by that of the electrons, and in this case, the expression for ω_P, N is the total number of electrons at m^3, q_P the elementary charge e and m_P the mass of electrons m_e.

Thus, if the angular frequency ω of the wave incident on the plasma is greater than that ωp of the plasma, then the wave vector $k > 0$ and the domain is said to be dispersive. In such a case, part of the wave will be reflected and the other propagates beyond the plasma without attenuation, with two types of velocities, one called the phase velocity and the other the group velocity. Indeed, an individual wave propagates at a speed called the phase velocity. However, if the wave results from the summation of several coherent waves called wave packets, the group velocity is the one that modulates the amplitude and is therefore almost independent of the angular frequency, while the phase velocity is the speed associated with the average of the individual wave vectors and is related to the phase. For example, consider a packet of coherent waves, that is, waves with almost the same angular frequency or frequency, comprising two waves, as in the case of our dual-frequency satellite with the same amplitudes:

$$\begin{cases} \overrightarrow{\mathrm{E_1}}(z,t) = \mathrm{E_0}.\cos(\omega_1.t - k_1.z)\overrightarrow{u_x}\,;\overrightarrow{\mathrm{E_2}}(z,t) = \mathrm{E_0}.\cos(\omega_2.t - k_2.z)\overrightarrow{u_x} \\ \vec{\mathrm{E}}(z,t) = \overrightarrow{\mathrm{E_1}}(z,t) + \overrightarrow{\mathrm{E_2}}(z,t) \rightarrow \\ \vec{\mathrm{E}}(z,t) = 2\mathrm{E_0}\cos\left[\left(\frac{\omega_1 - \omega_2}{2}\right)t - \left(\frac{k_1 - k_2}{2}\right)z\right].\cos\left[\left(\frac{\omega_1 + \omega_2}{2}\right)t - \left(\frac{k_1 + k_2}{2}\right)z\right]\overrightarrow{u_x} \end{cases}$$

So ω_1 near ω_2 so $\omega_1 - \omega_2 \cong 0$ and $\omega_1 + \omega_2 \cong 2\omega \rightarrow \omega \cong \omega_1 \cong \omega_2$ then the resulting wave will be of the form:

$$\vec{\mathrm{E}}(z,t) = 2\mathrm{E_0}\cos\left[\left(\frac{k_1 - k_2}{2}\right)z\right].\cos\left[\omega t - \left(\frac{k_1 + k_2}{2}\right)z\right]\overrightarrow{u_x} \quad (16)$$

Group speedV_g will be associated $(k_1 - k_2)/2$ and that of the phase V_p associated $(k_1 + k_2)/2$. However, in practice, the phase velocity and its index will be given by:

$$\begin{cases} V_p = \dfrac{\omega}{k} = \dfrac{C}{\sqrt{1 - \left(\frac{\omega_P}{\omega}\right)^2}} \rightarrow n_p = \dfrac{C}{V_p} = \sqrt{1 - \left(\frac{\omega_P}{\omega}\right)^2} \\ n_p = \sqrt{1 - \left(\frac{\omega_P}{\omega}\right)^2} \rightarrow n_p \cong 1 - \frac{1}{2}\left(\frac{\omega_P}{\omega}\right)^2 \rightarrow n_p \cong 1 - 40{,}3\frac{N}{f^2} \end{cases} \quad (17)$$

The group speed and its index will be given by:

$$\begin{cases} V_g = \dfrac{\partial\omega}{\partial k} = C.\sqrt{1 - \left(\frac{\omega_P}{\omega}\right)^2} \rightarrow n_g = \dfrac{C}{V_g} = \dfrac{1}{\sqrt{1 - \left(\frac{\omega_P}{\omega}\right)^2}} \\ n_g = \dfrac{1}{\sqrt{1 - \left(\frac{\omega_P}{\omega}\right)^2}} \rightarrow n_g \cong 1 + \frac{1}{2}\left(\frac{\omega_P}{\omega}\right)^2 \rightarrow n_p \cong 1 + 40{,}3\frac{N}{f^2} \end{cases} \quad (18)$$

The propagation time related to the phase and its variation will thus be described:

$$\begin{cases} \tau_p = \int \dfrac{ds}{V_p} = \dfrac{1}{C}\int n_p ds \rightarrow \tau_p = \dfrac{1}{C}\left[\int ds - \dfrac{40{,}3}{f^2}\int N.ds\right] \\ C.\Delta\tau_{p2,1} = C\left(\tau_{p2} - \tau_{p1}\right) = 40{,}3\left(\dfrac{1}{{f_1}^2} - \dfrac{1}{{f^2}_2}\right).\mathrm{TEC} \end{cases} \quad (19)$$

As for the groups, we obtain:

$$\begin{cases} \tau_g = \int \dfrac{ds}{V_g} = \dfrac{1}{C}\int n_g ds \rightarrow \tau_p = \dfrac{1}{C}\left[\int ds + \dfrac{40{,}3}{f^2}\int N.ds\right] \\ \Delta\tau_{p1,2} = \left(\tau_{g1} - \tau_{g2}\right) = \dfrac{40{,}3}{C}\left(\dfrac{1}{{f_1}^2} - \dfrac{1}{{f^2}_2}\right).\mathrm{TEC} \end{cases} \quad (20)$$

This method of determining the TEC is based essentially on the difference in code measurements $C\left(\tau_{p2} - \tau_{p1}\right)$ Equation 19, called the pseudo-frequency range f_1 and f_2 Ouattara et al., (2011), Zoundi et al., (2012), Ntumba

P. et al., (2012). These codes are contained in RINEX files, and a processing algorithm, as shown in Figure 6, has been proposed for this purpose Fleury R., (2017).

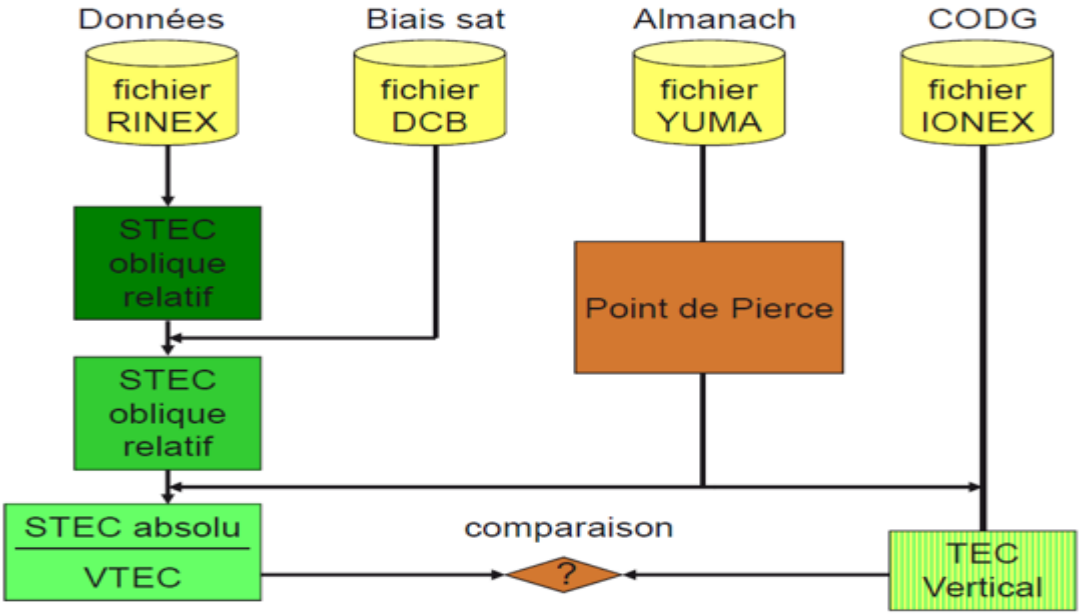

Fig.6. TEC processing algorithm Fleury R., (2017).

The TEC thus obtained is the STEC which will be corrected to VTEC taking into account the satellite biases provided by CODE (Center for Orbit Determination Europe) and the receiver bias determined by comparing the results of the model provided by CODE (CODG) with the in situ measurements.

5.2. Approach using analytical calculations of VTEC and STEC by altitudinal integration

The methodology section demonstrated the process of obtaining VTEC and STEC, and the diurnal modeling of these values shows exponential growth at 6 AM, 12 PM, 6 PM, and midnight. These exponential values are justified because these times represent periods of uncertainty. On the one hand, the densification surface should be non-zero, but it is at 6 AM and 6 PM, within a few decimal places. The same applies to 12 PM and midnight, where the velocity (Vz), which should not be zero, is also non-zero at noon and midnight, within a few decimal places. How can this be resolved? Does this mean that we would observe VTEC maxima at these times and at any geographical location? To address this, in the following sections, we will propose hypotheses and approximations capable of resolving this, but which will remain, or appear in this respect, as limitations.

5.2.1. VTEC issues during the hours of 6 AM and 6 PM

Observation of both measured and modeled TEC variability curves shows that TEC variability is complex. Besides geographical location, this variability is a function of the seasons, the solar cycle, and, for the same cycle, TEC variability depends on the phase of the cycle. The TEC variability observed at 6 AM and 6 PM is not always at its maximum. At times, minimums or other values are observed, as illustrated in the figures below:

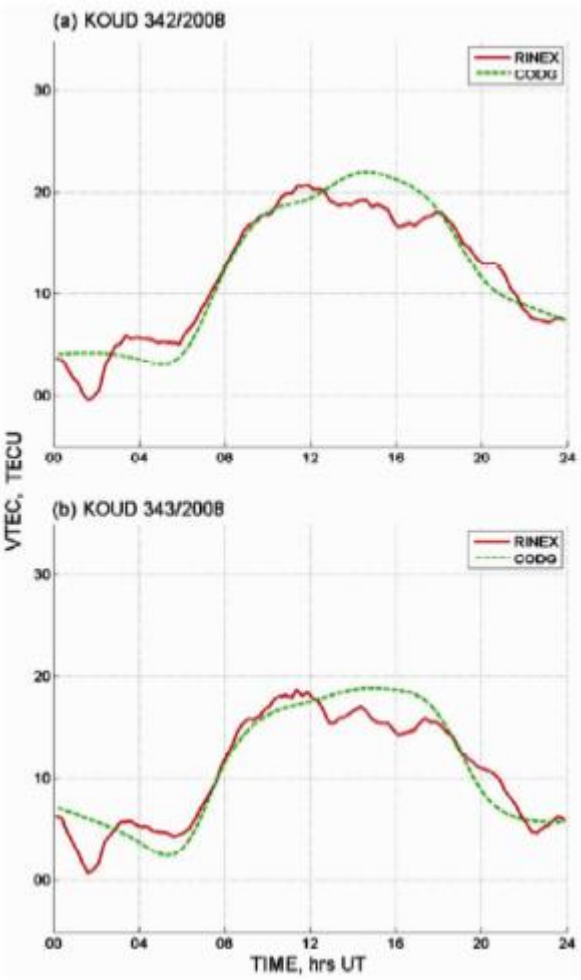

Local time variation of RINEX TEC and map TEC for: (a) 7 December 2008 and (b) 8 December 2008. Zoundi et al., (2012).

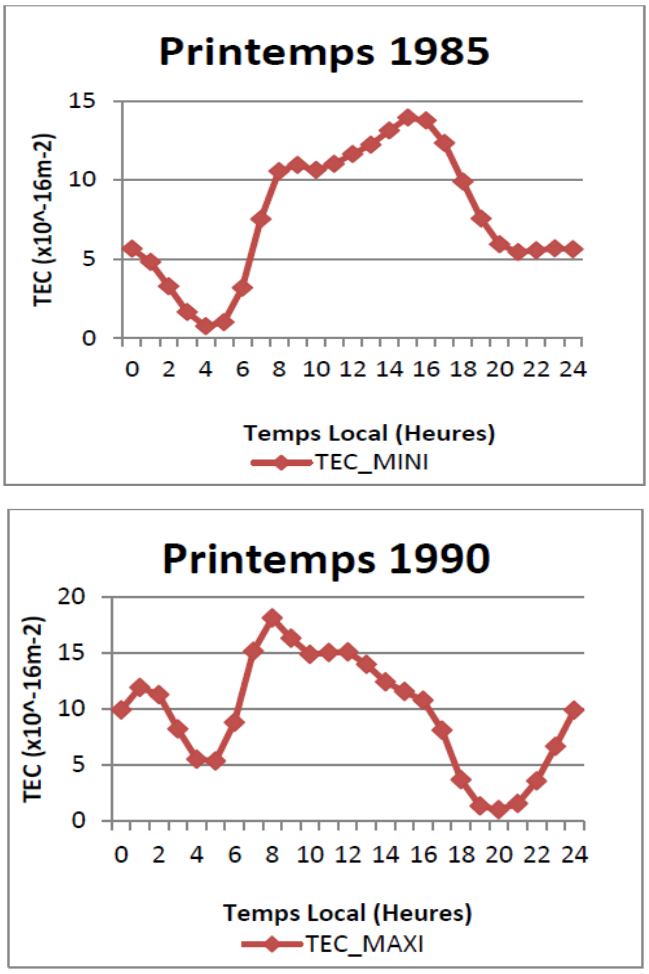

Local time variation of IRI 2016 TEC and map TEC for Spring 1985 (March) and Spring 1990 (March). Ilboudo et al., (2021)

Fig. 7. Variability of the TEC in different years and periods of the year by RINEX and by IRI 2016

To resolve this in the proposed model, since the volume is zero and the only non-zero parameters at these times are the speeds Vx, Vy and Vz then we will consider the W.s³/m³ that is, the power of solar radiation divided by the product of the velocity coordinates. For this, the variations at 6 AM and 6 PM will only be considered for the latter.

$$\begin{cases} \dfrac{d(V_xV_yV_z)}{dz} = \dfrac{d(V_xV_yV_z)}{dt}.\dfrac{1}{V_z} = \dfrac{(a_xV_y + V_xa_y)V_z + V_xV_ya_z}{V_z} \\ \dfrac{d(V_xV_yV_z)}{dz} = (a_xV_y + V_xa_y) + \dfrac{V_xV_ya_z}{V_z} \end{cases}$$

$$(V_xV_yV_z)(z) = (z - z_0)\left[(a_xV_y + V_xa_y) + \frac{V_xV_ya_z}{V_z}\right]_{t0} + (V_xV_yV_z)(z_0)$$

$$\text{VTEC U}(\Delta z) = 42{,}38 \int_{z1}^{z2} \frac{\left[\frac{h}{V_z}\right]_{t0}(z - z_0) + kP0(z_0)}{\left[(z - z_0)\left[(a_xV_y + V_xa_y) + \frac{V_xV_ya_z}{V_z}\right]_{t0} + (V_xV_yV_z)(z_0)\right]} dz$$

The integration that produces VTEC takes the form:

$$\begin{cases} \int_{z1}^{z2} \frac{az+b}{cz+c}\,dz \\ a = \left[\frac{h}{V_z}\right]_{t0} \rightarrow b = kP0(z_0) - \left[\frac{h}{V_z}\right]_{t0} z_0 \\ c = \left[(a_x V_y + V_x a_y) + \frac{V_x V_y a_z}{V_z}\right]_{t0} \rightarrow d = V_{(x,y,z)}(z_0) - \left[(a_x V_y + V_x a_y) + \frac{V_x V_y a_z}{V_z}\right]_{t0} z_0 \end{cases}$$

$$\text{VTEC U}(\Delta z) = \left(\frac{42{,}38}{c}\right).\left(\left[(az_2+b) - a\left(\frac{cz_2+d}{c}\right)\right] ln|cz_2+d| + \left[a\left(\frac{cz_1+d}{c}\right) - (az_1+b)\right] ln|cz_1+d| + a(z_2-z_1)\right) \quad (21)$$

We obtain the following graph Figure 8 below where the value at 12H is taken as zero but whose VTECU values at 6H and 18H are no longer zero but 3.27 TECU.

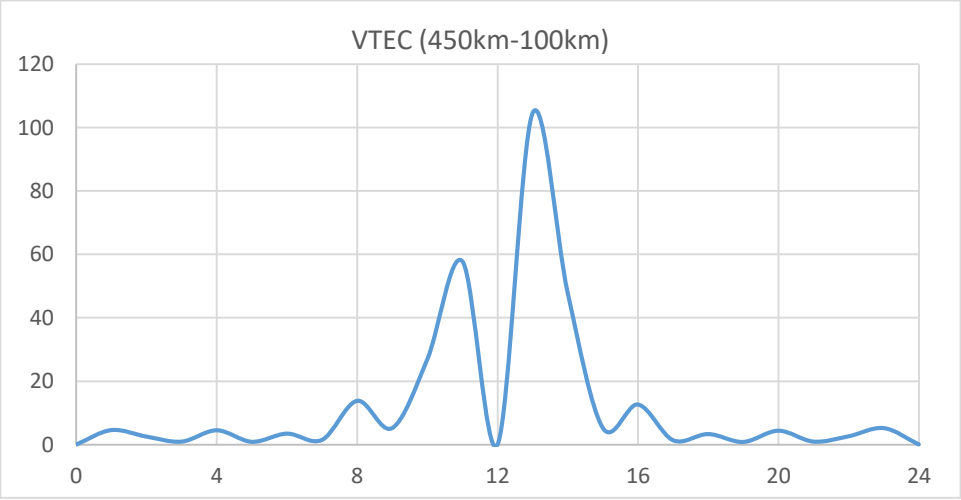

Fig. 8. The problem at 6 AM and 6 PM, where the values found were exponential, is now 3.27 TECU. Lat 13° and long 358°

5.2.2. Problem of VTEC hours at 12 PM

The problem at 12:00 PM, where the velocity Vz becomes zero, could be resolved by assuming that 12:00 PM is the median time and that the altitudinal variation of the power density at 12:00 PM is such that the h' at 12:00 PM is the average of the h' values during the day. This ultimately yields the following graph, where the value at 12:00 PM is now 42.34 TECU:

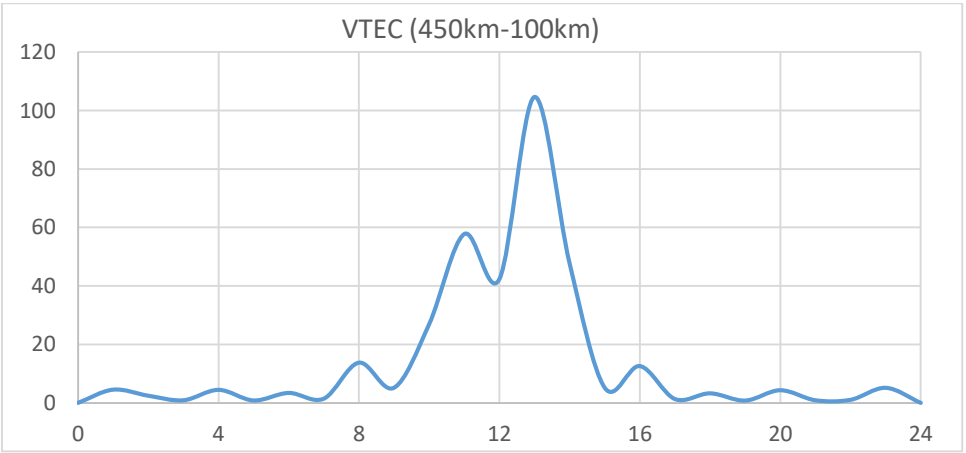

Fig. 9. LAT 13° - LONG 358° The value at 12:00 is now 42.34 TECU

The following graph is obtained exactly at the position of the Koudougou station (Lat 12°15'N, Long -2°20'E):

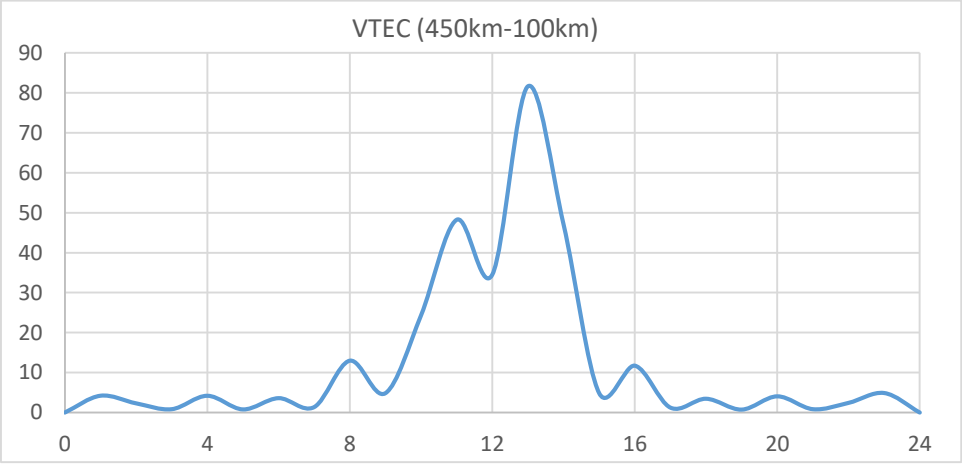

Fig. 10. Variability of the TEC at Koudougou Lat 12.25°N, Long 357.67°E

Thus, the diurnal variation of VTEC obtained shows a profile with nighttime minima from 6 PM until the early morning hours, when a resurgence in VTEC amplitude begins to be observed. This increase in VTEC amplitude culminates at the end of the day in a Noon Bit Out type profile, also known as profile B, characterized by two asymmetrical peaks: one in the morning at 11 AM and the other in the afternoon at 1 PM, separated by a trough at noon. According to Vassal et al., 1982, such a profile can be interpreted as follows: the morning peak is due to the presence of an electrojet (Chapman et al., 1951), the evening peak to a counter-electrojet, and the trough to the vertical drift resulting from the intersection of the zonal electric field and the horizontal magnetic field. For Segda et al, (2025), (2026), the equatorial electrojet is hypothetical; the observed peaks are production peaks where the solar rays are more penetrating, and the trough is due to the vertical drift, i.e., less production where the sun's rays are no longer very penetrating because they are reduced in power. In comparison, the profile observed using altitudinal calculations contrasts somewhat with that observed using RINEX data (Figure 7a above), where the observed profile is dome-shaped, indicating the absence of both over- and under-projection. Conversely, with IRI 2016 (Figure 7b), a VTEC profile of the Reversed or R type is observed in spring 1985, and a Morning Peak or M type in spring 1990. According to Vassal et al., 1982, such R and M profiles are interpreted respectively by the presence of strong under-projection in the evening and strong over-projection in the morning. For Segda et al., 2025, the R profile is characterized by the clear predominance of the afternoon production peak over the morning peak, and the M profile by the morning peak over the evening peak. Also, the VTEC values obtained, with a maximum of around 80 TECU compared to 30 TECU with the RINEX data, will be assigned the chosen average vertical drift speed of around 20.58 m.s-1. Another chosen speed, as shown in the following section, could further increase or decrease the VTEC values.

5.2.3. Factors affecting VTEC variability

The formula thus obtained eliminates the exponential values observed at 6 AM, 12 PM, 6 PM, and midnight. We can therefore observe that for the same longitude, the profile remains identical, but that the VTEC increases in amplitude from the equator to the poles. For the same latitude, we obtain diverse profiles depending on the longitude, and at certain positions at 12 PM, we observe maxima in VTEC values, further reinforcing the proposed formula. Also (Figure below), at 11 AM for the city of Fada N'Gourma, located at the geographic position Lat 12.05°N, Long 0.35°E, we observe that the VTEC is at its maximum.

5.2.3.1. Impact de la vitesse de dérive verticale et facteur k sur la variabilité du VTEC

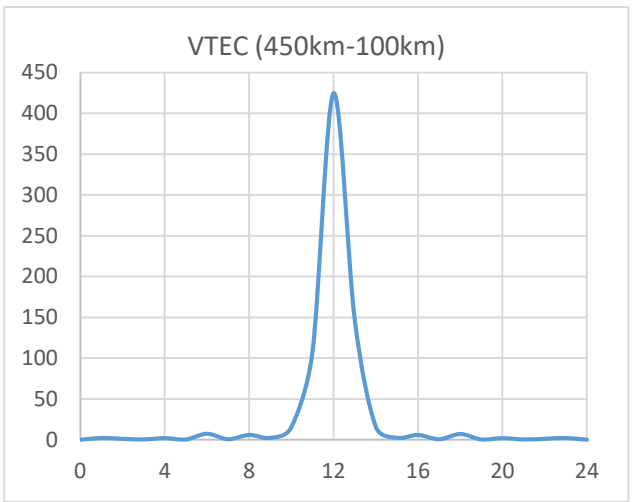

Lat 13°-Long 180°E: Vmoy=20,57m.s^{-1}, k= 536,73 W.m^{-1}

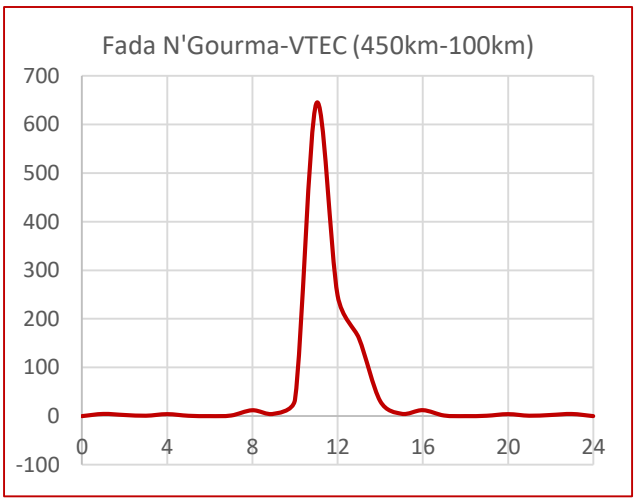

Lat 12,05°-Long 0,35°E: Vmoy=20,57m.s^{-1}, k= 268.61W.m^{-1}

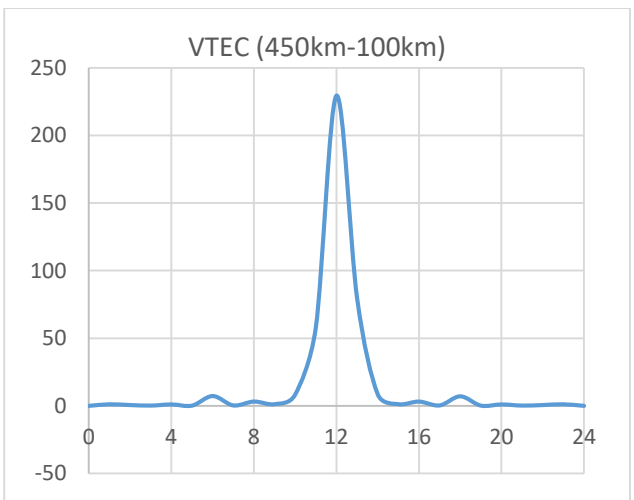

Lat 13°-Long 180°E: Vmoy=28 m.s^{-1}, k= 730,26 W.m^{-1}

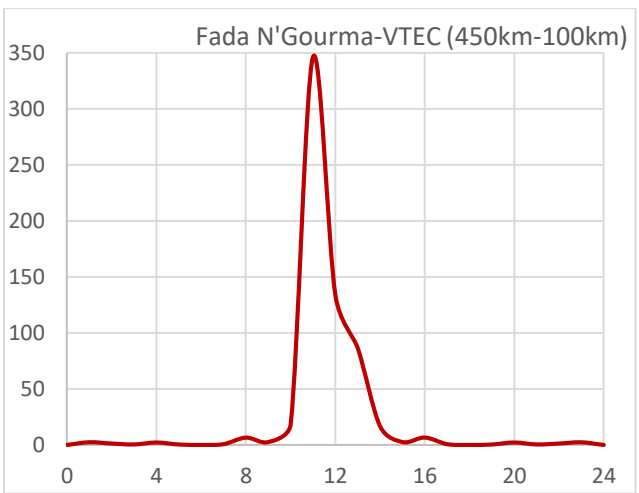

Lat 12,05°-Long 0,35°E: Vmoy=28 m.s^{-1}, k= 365,64

Fig.11. TEC variability showing the impact of vertical drift velocity parameters and ionization production factor at Fada N'Gourma (Lat 12.05°N-Long 0.35°E) and at Lat 13°N, Long 80°E.

Thus, we observe that for the same geographical location, the higher the ionization velocity or vertical drift, the higher the production factor k and the lower the VTEC. Conversely, the lower the ionization velocity or vertical drift, the lower the production factor k and the higher the VTEC.

5.2.3.2. Variation latitudinale du VTEC

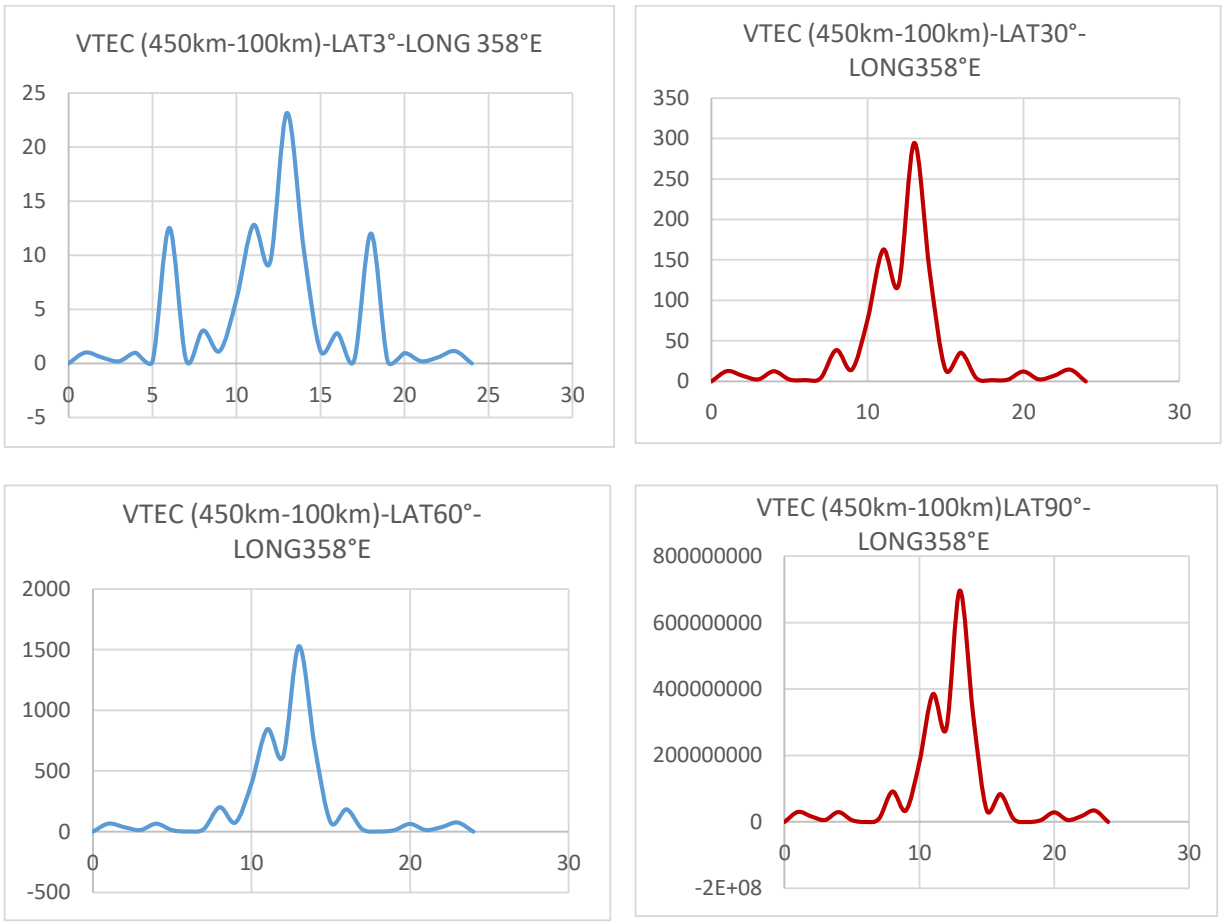

Fig.12. Variability of the TEC as a function of latitude for a fixed longitude.

The latitude variations in VTEC show an equatorial ionization anomaly between 6 AM and 6 PM. This anomaly is inverse. VTEC values at these times are highest at latitudes increasingly closer to the equator and decrease with distance from the equator. During the day, an increase in VTEC is observed from the equator to the poles, where the observed values are exponential, suggesting that this could explain the auroras (northern and southern lights) observed at these latitudes, which are often attributed to the precipitation of energetic particles by polar cusps.

5.2.3.3. Longitudinal variation of VTEC

Unlike altitudinal variation, which maintains the VTEC variability profile, longitudinal variations show a diversity of profiles for the same latitude but different longitudes. We can therefore deduce that VTEC profiles are rigid in terms of latitude but flexible with regard to longitude.

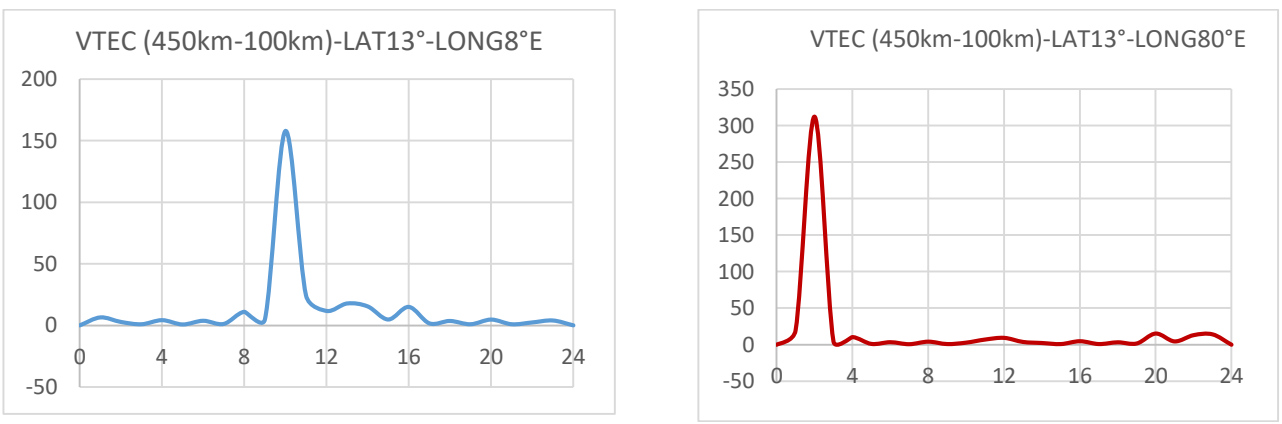

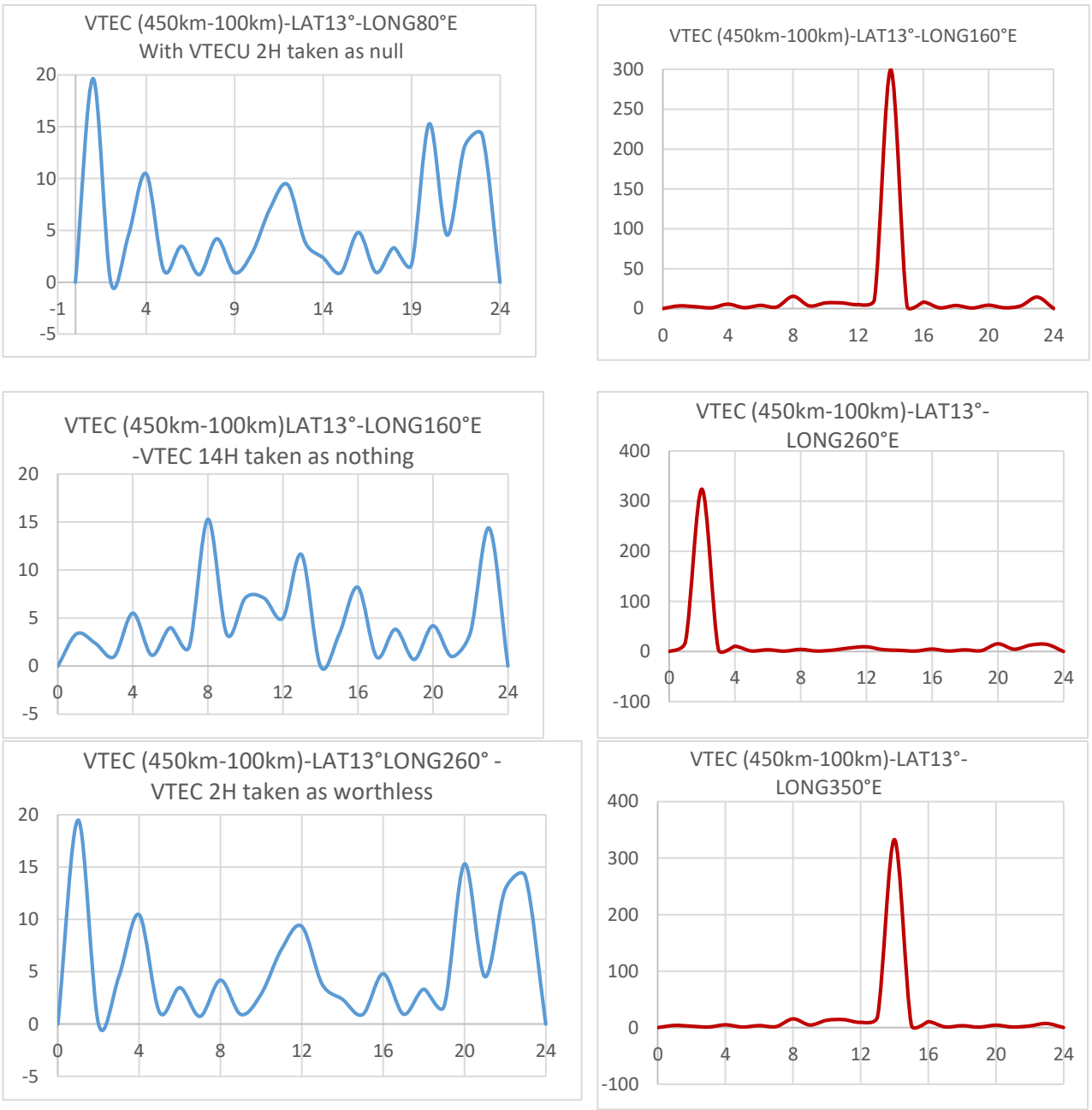

Fig.13. Variability of the TEC as a function of longitude for a fixed latitude.

5.3. STEC Profile

As mentioned above, the STEC profile will be given by applying the formula:

$$VTEC = \left[1 - \left(\frac{\cos e}{1 + \frac{h}{R_T}}\right)^2\right] STEC \rightarrow STEC = \frac{VTEC}{\left[1 - \left(\frac{\cos e}{1 + \frac{h}{R_T}}\right)^2\right]}$$

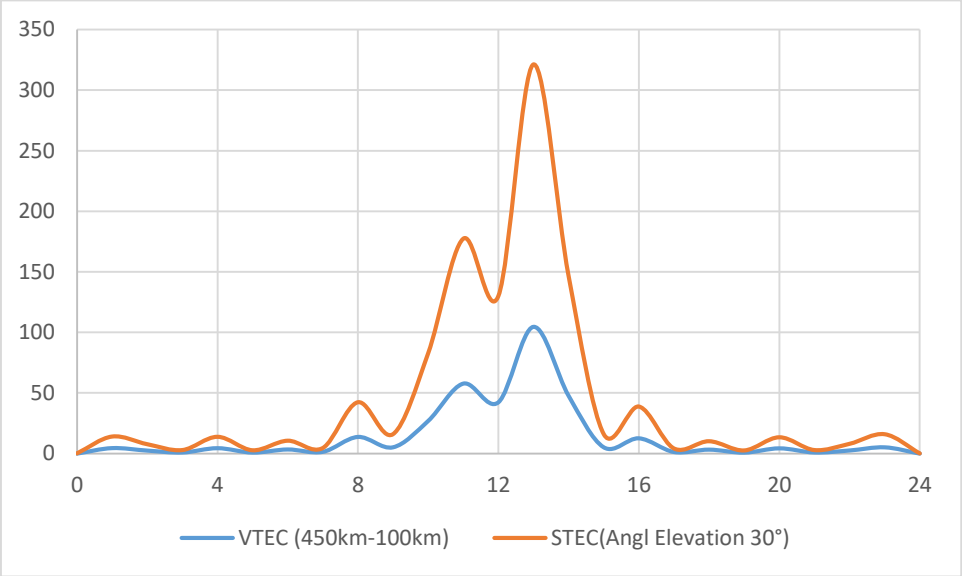

Fig. 14. VTEC and STEC variability at LAT 13° LONG 358° elevation angle 30°

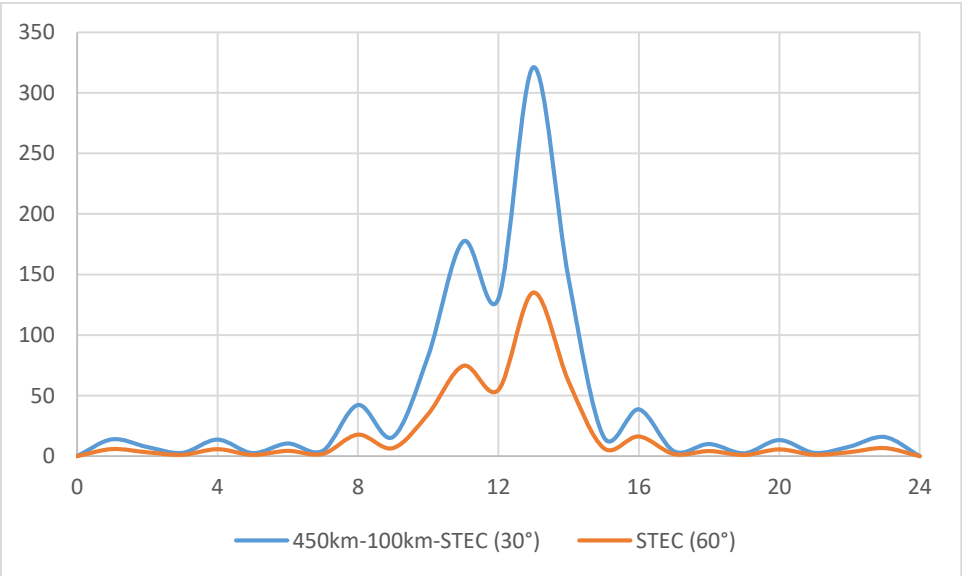

Fig. 15. Variability of STEC as a function of the elevation angle LAT 13° Long 358°

From observing these variability curves, we can deduce that the greater the angle of elevation, the more the STEC decreases.

5.4. Importance of the study

This manuscript addresses an important problem in ionospheric physics, namely the analytical determination of Total Electron Content (TEC), which is critical for GNSS applications and space weather studies. The proposed theoretical framework, based on altitudinal integration of solar radiation power density, represents an interesting attempt to provide an alternative to empirical and data- driven models such as IRI or NeQuick. The work could be valuable if further validated, as it aims to enable TEC estimation at any geographical location without dependence on observational datasets. However, the current version still requires significant refinement in terms of physical justification, validation, and clarity before it can be considered a strong contribution to the field. Also of importance, we have the following other applications:

5.4.1. Variation of critical frequencies

Critical frequencies are defined as the maximum reflection frequencies on an ionospheric layer. For the F2 subshell, for example, the critical frequencies in hertz are denoted foF2 and given by the expression below, where N is the electron density per cubic meter:

$$foF2 = 8{,}96.\sqrt{N} \quad (22)$$

Thus, knowing the electron density for a given altitude, we can deduce the diurnal variability of the critical frequencies foF2 at any geographical location. As a reminder, the volume density of electrons at a given altitude is given by the expression:

$$\begin{cases} \text{VTEC U}(\Delta z) = \left(\frac{42{,}38}{3600}\right) \int_{z1}^{z2} \frac{\left[\frac{h}{V_z}\right]_{t0}(z - z_0) + kP0(z_0)}{\left[(z - z_0)\left[\frac{dS(x,y)}{dz}.z + S(x,y)\right]_{t0} + V_{(x,y,z)}(z_0)\right]} dz \\ \text{VTEC U}(\Delta z) = \int_{z1}^{z2} N\, dz \rightarrow N = \left(\frac{42{,}38}{3600}\right) \frac{\left[\frac{h}{V_z}\right]_{t0}(z - z_0) + kP0(z_0)}{\left[(z - z_0)\left[\frac{dS(x,y)}{dz}.z + S(x,y)\right]_{t0} + V_{(x,y,z)}(z_0)\right]} \end{cases}$$

Since N is in TECU.m^{-3}, i.e., 10^{16} electrons.m^{-3}, then from this expression we deduce the formula giving the variation of foF2:

$$\begin{cases} foF2(z)_{Hz} = 8{,}96.\sqrt{\left(\frac{42{,}38}{3600}\right).10^{16}.\left|\frac{\left[\frac{h}{V_z}\right]_{t0}(z - z_0) + kP0(z_0)}{\left[(z - z_0)\left[\frac{dS(x,y)}{dz}.z + S(x,y)\right]_{t0} + V_{(x,y,z)}(z_0)\right]}\right|} \\ for\ z \rightarrow \infty \\ foF2(z)_{Hz} = 8{,}96.\sqrt{\left(\frac{42{,}38}{3600}\right).10^{16}.\left|\frac{\left[\frac{h}{V_z}\right]_{t0}}{\left[\frac{dS(x,y)}{dz}.z + S(x,y)\right]_{t0}}\right|} \end{cases} \quad (23)$$

For example, at the geographical positions LAT 13°N and LONG 358°E, LAT 1°N LONG 38°E and at an altitude of 350 km, the following variations in foF2 are obtained (Figure 16):

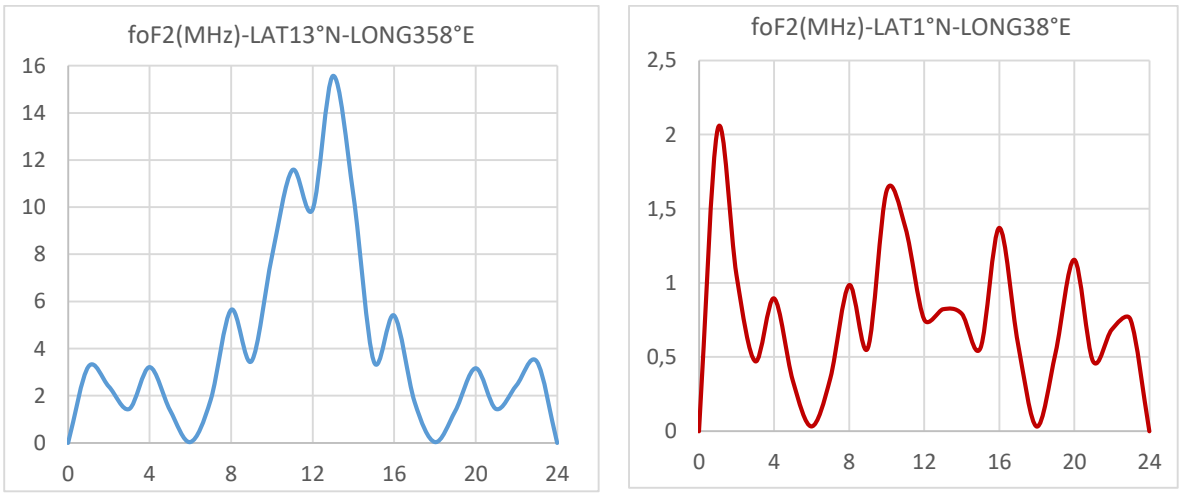

Fig. 16. Variability of critical frequencies exhibiting different profiles

5.4.2. Current densities

Knowing the volume density of electrons as well as the different components of the velocity vector of the ionization densification surface we can deduce the electric current density at a given altitude as well as these different components.

$$\vec{J} = N.q.\vec{V} \rightarrow J = N.V \; and: \begin{cases} J_x = N.q.V_x \\ J_y = N.q.V_y \\ J_z = N.q.V_z \end{cases} \quad (24)$$

For example, at the geographical position LAT 13°N and LONG 358°E and at an altitude of 350 km, the following variation in current densities in A.m-2 is obtained:

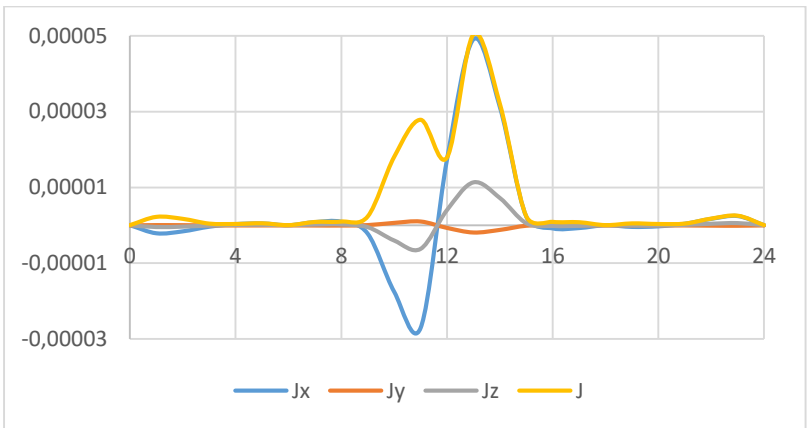

Fig. 17. Current densities at LAT 13°N and LONG 358°E

Finally, an example of variation in critical frequencies and current densities of six West African countries (Figure 18 below) shows that the peak times of current densities are also the peak times of critical frequencies.

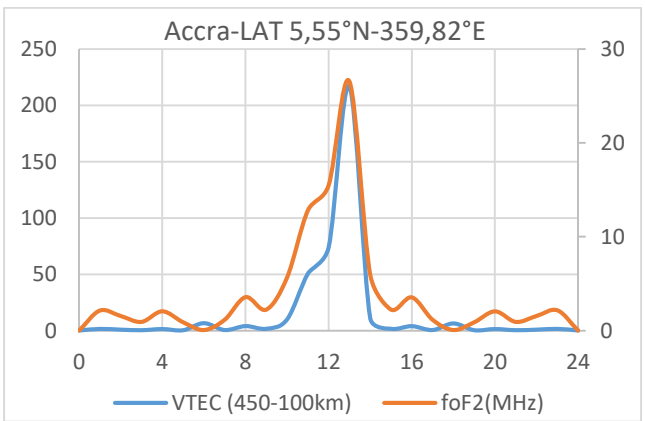

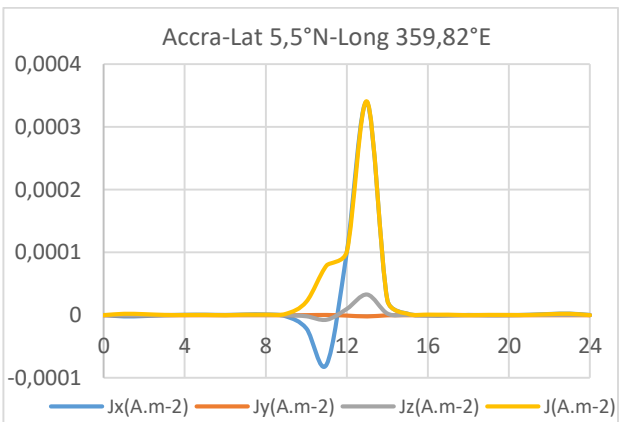

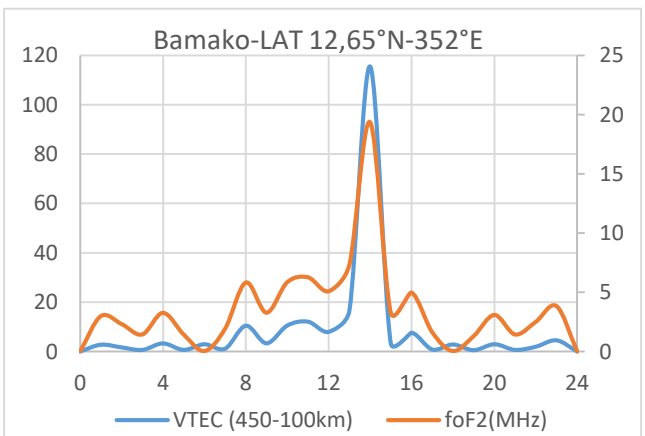

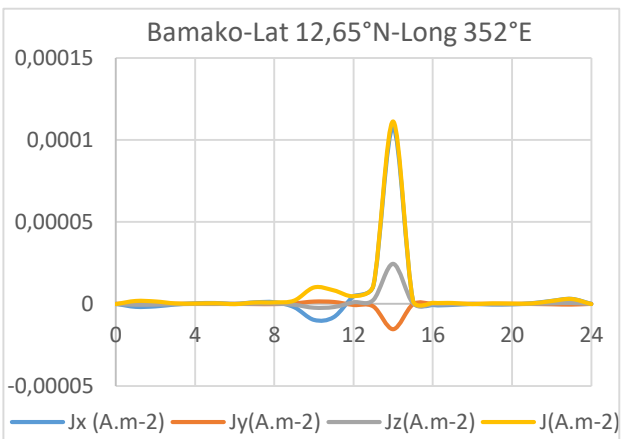

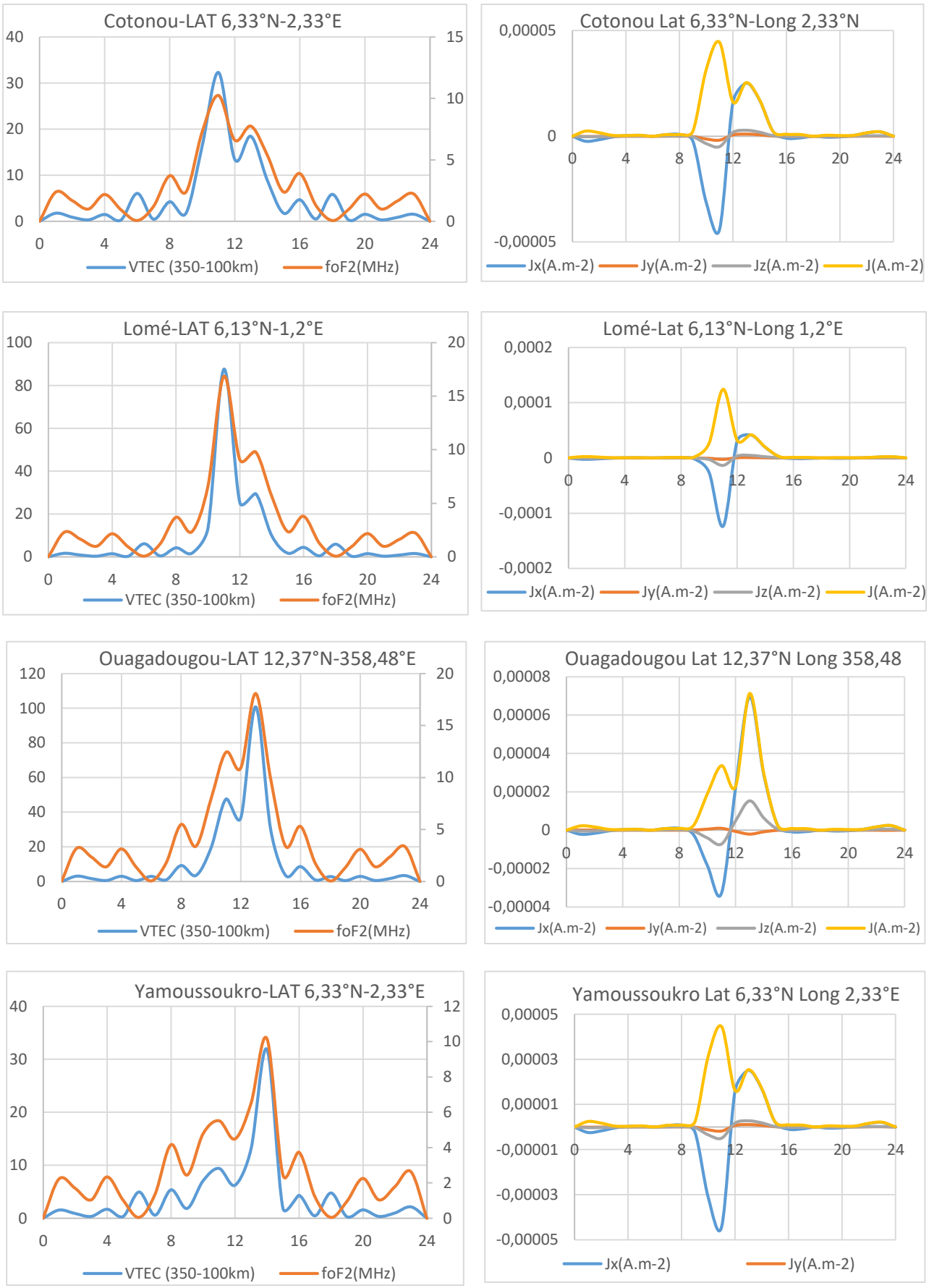

Fig.18. Example of variability of critical frequencies and current density for different cities in West Africa.

5.4.3. Seasonal variations

VTEC and STEC variations, in addition to latitude, longitude, and altitude, are also linked to vertical drift or ionization velocity via the production factor. Seasonal studies are then possible using the average ionization velocity. Thus, using satellite data such as that from Jicarmarca or others like IRI 2020, or by considering a city very close to the equator, we can deduce the values for all other geographical locations and consequently determine the ionization factor k, which in turn allows us to understand the seasonal variability of other parameters such as VTEC, STEC, foF2, current densities, etc.

5.5. Limitations of the study

The hours 6 AM, 12 PM, 6 PM, and 12 AM showed indeterminacies because Vz was zero to within a few decimal places, as was the ionization densification surface. Exponential values were observed at these times. Approximate calculations were then undertaken. Also as a limit, the average speed of vertical drift is chosen to be identical at any geographical position and only the factor of production varies because it also depends on the geographical latitude.

5.6. Perspectives

As a perspective we will study the northern and southern lights, the maximum heights of critical frequencies, scintillations, electric and magnetic fields etc.

6. Conclusion

Following the completion of this article, the objective of analytically calculating VTEC and STEC by altitudinal integration of solar radiation power density has been achieved. To this end, a formula for modeling the diurnal variability of VTEC and STEC is proposed. This formula is derived from the integration of the electron volume density, which itself is the product of the solar radiation power density and the number of electrons, taking into account the ionization energy of the oxygen atom. After refining the formula for the hours 6:00 AM, 12:00 PM, 6:00 PM, and 12:00 AM, which exhibited exponential values, the VTEC and STEC models revealed a variability profile that is a function of geographical location, with some specific characteristics. The variability profile is rigid in terms of latitudinal variability for a fixed longitude and flexible along longitudes for a fixed latitude. Indeed, the profile remains constant across latitudes, and only the amplitudes vary. The maximum VTEC values are reached between 6 AM and 6 PM at the equator, gradually decreasing to zero around latitudes of 10°N, S to 20°N, S. At other times of day, the amplitudes increase with distance from the equator. Depending on the longitude, the profiles are atypical, and a given time can record the maximum VTEC value at any given location. The same observations made with VTEC will also be true for STEC, which has also shown that the greater the elevation angle, the lower the STEC values. Other important aspects of the study, besides VTEC and STEC, include the fact that knowing the electron volume density allows us to deduce the formulas for the variability of critical frequencies and the electric current density. Knowing the surface density of electrons, its altitudinal integration has allowed us to highlight another form of VTEC which is expressed not in TECU, whose unit is 1016 electrons per m2, but in TECU, whose unit is 1016 electrons per m. After showing that it is possible to carry out models according to the seasons by the production factor or the vertical drift velocity, given the limits, the study concludes with the formulation of many perspectives.

Disclaimer (Artificial Intelligence)

Author(s) hereby declare that NO generative AI technologies such as Large Language Models (ChatGPT, COPILOT, etc) and text-to-image generators have been used during writing or editing of this manuscript.

Competing Interests

Authors have declared that they have no known competing financial interests OR non-financial interests OR personal relationshipsthat could have appeared to influence the work reported in this paper.

References

Banks, P. M., R. W. Schunk, and W. J. Raitt (1976), The topside ionosphere: A region of dynamic transition, Annl. Rev. Earth Planet. Sci., 4, 381.

Fleury R., Fichiers IONEX/CODG cartographies GIM, IMT Atlantique, Campus de Brest, France, 2017.

Fleury R., Traitement des données GPS, le fichier RINEX, IMT Atlantique, Campus de Brest, France, 2017.

Fleury R., Traitement fichiers GPS, Fichiers YUMA, IMT Atlantique, Campus de Brest, France, 2017.

Fleury R., Traitement mesures GPS, RINEX & fichiers DCB, IMT Atlantique, Campus de Brest, France, 2017.

Frédéric O., Christian Z., Christine AM., Rolland F., Patrick LD (2011). Détermination du contenu électronique total à partir des pseudo distances (PD) ou pseudo range (PR) à la station de Koudougou au Burkina Faso. J. Sci.Vol. 11, N° 1 (2011) 12– 19.

Frédéric O., Christian Z., Rolland F., (2012) Comparison between CODG TEC and GPS based TEC observations at Koudougou station in Burkina Faso. Indian Journal of Radio, Space Physics. Vol 41, December 2012, pp 617-623

J. Vassal, "The variation of the magnetic field and its relations with the equatorial electrojet in eastern Senegal", Annales de Géophysique, vol. 38, pp. 347–355, 1982.

Karia, S.P., et al. (2014) Modification in Atmospheric Refractivity and GPS Based TEC as Earthquake Precursors. Positioning, 5, 46 52. http://dx.doi.org/10.4236/pos.2014.52006

Ntumba P. et al., Développement et déploiement d'une application « desktop » et mobile sur une mini grille de calcul à l'Université de Kinshasa pour le traitement des données GPS. Colloque à l'université de Kinshasa, RDC, 2012.

Phyo C Thu , Pornchai Supnithi , Jirapoom Budtho ,Apitep Saekow,Thanomsak Sopon, Kornyanat Hozumi , and Lin Min Min Myint , Non-members. (2023). Instrumental Receiver Bias Estimation for Ionospheric Total Electron Content by Neural Network Model. https://creativecommons.org/licenses/by-nc-nd/4.0/. Digital Object Identifier:10.37936/ecti-eec.2023213.251470

Raoul ILBOUDO, Emmanuel NANEMA, Frédéric OUATTARA (2021). Vol. 40, n° 2 – Juillet - Décembre 2021 Science et technique, Sciences Naturelles et Appliqué.

Rishbeth, H., et al. (2000). The equinox transition in the ionosphere. *Annales Geophysicae*, 18, 285–299.

S. Chapman, "The equatorial electrojet as detected from the abnormal electric current distribution above Huancayo, Peru, and elsewhere," Archiv Fuer Meteorologie, Geophysik und Bioklimatologie, Serie A, vol. 4, no. 1, pp. 368–390, 1951.

S. Sunda, BM Vyas, SV Satish et KS Parikh, « Amélioration de la précision de position avec GAGAN et impact deScintillation sur GNSS », Positioning , Vol. 4 No. 4, 2013, pp. 282-288. Published Online November 2013 (http://www.scirp.org/journal/pos) http://dx.doi.org/10.4236/pos.2013.44028

Scherliess, L., & Fejer, B.G. (1999). Radar and satellite global equatorial F region vertical drift model. *Journal of Geophysical Research : Space Physics*, 104(A4), 6829–6842.

Segda Abdoul-Kader, Gnabahou Doua Allain and Kaboré Salfo (2023a) Contribution to the explanation of the semi-annual anomaly observed in the intertropical zone using the critical frequencies fof2 extracted during the sunspot cycles 20, 21 and 22 at the Ouagadougou. International Journal of Advanced Research. http://dx.doi.org/10.21474/IJAR01/16266

Segda Abdoul-Kader, Gnabahou Doua Allain and Gyebré Aristide (2023b) New Analysis of the Seasonal Variation of the Critical Frequencies foF2 by a Proposed Formula of the Power of Solar Radiation. International Journal of Geophysics. *1687-885X/1687-8868.* https://doi.org/10.1155/2023/4405266

Segda, A.K., Kabore, S., Gybre, A., Saidou, M. and Ouattara, F. (2025) Analysis and Estimation of the Vertical Drift Velocity from the Ionization Production Velocity in Correspondence with Radar Data from Jicamarca and IRI 2020. Journal of Applied Mathematics and Physics, 13, 2674-2691. https://doi.org/10.4236/jamp.2025.138152

Segda, A.K., Kabore, S., Gybre, A.M.F., Belemlilga, D., Obrou, K.O. and Ouattara, F. (2026) Analysis of the Spatio-Temporal Variability of the Solar Quiet Sq/Sr Ionospheric Currents of the Equatorial EEJ and CEJ/REJ Electrojets by the Ionization Densification Surface. International Journal of Geosciences , 17,183-214. https://doi.org/10.4236/ijg.2026.173010

Zoundi C. et OUATTARA F. Process for determining Total Electron Content (CET) (2012). Rev. CAMES-Série A, 13(2):139-143.